Double dissociation of sensorimotor interaction mediated by visual feedback during continuous *de novo* motor learning

Short Title: Double dissociation of sensorimotor interaction

Authors: Junghyun Kim[1], Sungbeen Park[2], Kwangsun Yoo[3,4], Sungshin Kim[1,2,5]*

1. Department of Data Science, Hanyang University, Seoul, Republic of Korea
2. Department of Artificial Intelligence, Hanyang University, Seoul, Republic of Korea
3. Department of Digital Health, Samsung Advanced Institute for Health Sciences and Technology (SAIHST), Sungkyunkwan University (SKKU), Seoul, Republic of Korea
4. Data Science Research Institute, Research Institute for Future Medicine, Samsung Medical Center, Seoul, Korea
5. Center for Neuroscience Imaging Research (CNIR), Institute for Basic Science (IBS), Suwon, Republic of Korea

keywords: motor skill learning, fMRI, visual feedback

*Corresponding Author
#505, Fusion Tehchnology Center,
222 Wangsimni-ro Seongdong-gu, Seoul, Republic of Korea
Email: sungshinkim@hanyang.ac.kr
Phone: +82-10-4687-5322

Data Availability

All MRI data used in this study are archived in the Hanyang University Network Attached Storage (NAS). The corresponding author can provide any information on the dataset related to this study if necessary.

Funding

This work was supported by the National Research Foundation of Korea (NRF-2021R1A2C2011648), Hanyang University (HY-202000000002753), and Center for Neuroscience Imaging Research, Institute for Basic Science, Korea (IBS-R015-D1).

Conflict of Interest

The authors declare that there is no conflict of interests.

Ethics Approval Statement

All participants provided written consent in accordance with the dictates of the trust ethics committee of Sungkyunkwan University, Suwon, Republic of Korea.

Acknowledgments

Neuroimaging was performed at the Center for Neuroscience Imaging Research located in Sungkyunkwan University, supported by Institute for Basic Science.

Abstract

While the sensorimotor cortices are central neural substrates for motor control and learning, how interaction between their subregions with visual cortices contribute to acquiring *de novo* visuomotor skill is poorly understood. We designed a continuous visuomotor task in fMRI where participants learned an arbitrary visuomotor mapping. To dissociate functions of motor and somatosensory cortices, we manipulated visual feedback of a cursor that they learned to control using fingers under two alternating conditions: online cursor feedback is available or unavailable except when a target is reached. We found double dissociation of fMRI activity in subregions of the sensorimotor and visual cortices and their interaction, which were mediated by the visual feedback. We also found significant reduction in functional connectivity between somatosensory cortices and early visual cortices, which was highly correlated with performance improvement. These findings support the distinct interaction between subregions of sensorimotor cortices and visual cortices while highlighting the more dominant role of somatosensory cortices over motor cortices during *de novo* motor learning.

Introduction

Visuomotor learning involves execution and correction of motor commands to achieve a task goal based on visual feedback, which is underpinned by adaptive interaction between sensorimotor and visual cortices[1,2]. It has been well established that the visual feedback shapes visuomotor learning while modulating activities of neural substrates engaged in the visuomotor interaction[3-7]. For instance, we can manipulate visibility of the feedback providing continuous movement of the end-effector or its position only at the end of movement[3,8,9]. The visibility could affect integration of the visual feedback with other sensory feedback such as proprioception, which is processed by the somatosensory cortices. Additionally, the visibility also could distinctively modulate activity in early and late visual cortices as well as their interaction with sensorimotor cortices. Thus, manipulation of visual feedback could be a promising approach to investigating distinct functional roles of the sensorimotor and visual subregions in visuomotor learning.

However, the motor and somatosensory cortices are often coactivated during motor task, as reported in previous fMRI studies using a similar manipulation of the visual feedback[8-11]. The coactivation would be primarily due to intricate interaction between motor and somatosensory cortices during movement[7]. The motor and somatosensory cortices are closely interconnected, playing roles in creating motor commands, anticipating sensory outcomes, and processing sensory feedback. The intertwined interaction makes it challenging to determine the extent to which motor versus somatosensory cortices contribute to motor learning[7]. Previous studies employed simple motor control tasks such tracking a target[8], moving a pendulum[9], and hand-grasping task[10,11], in which they have not investigated neural plastic changes of the sensorimotor network. Moreover, little has been explored how the subregions of the sensorimotor network interact with those of the visual network, early and late visual cortices.

Here, we employed a fine motor skill learning task in fMRI where participants use their fingers to control an on-screen cursor while learning an arbitrary hand-to-cursor mapping[12]. In

contrast to typical motor adaptation and sequence learning tasks with well-defined sensory targets, our task requires exploration in a high dimensional motor space while learning proprioceptive state, i.e., hand posture, which is mapped to a low dimensional target space. Given that the afferent proprioception is critical in the task, we sought to disentangle its role in motor learning from that of efferent motor execution. Furthermore, we hypothesized that their neural substrates, motor cortices and somatosensory cortices would differentially interact with visual cortices during motor learning. To this end, we manipulated visibility of the visual feedback so that participants performed a motor learning task under two interleaved feedback conditions with full online visual feedback of the cursor movement and visual feedback only available when the cursor reached a target otherwise hidden. We first contrasted the overall fMRI activity in the motor and somatosensory cortices as well as that in the subregions of the visual cortices for the two visual feedback conditions. Then, we further explored the functional connectivity patterns between the sensorimotor and visual networks and correlated them with learning performance.

Results

Behavioral data analysis

Twenty-four participants completed the experiment. The main task began after the localizer session. The purpose of localizer session was to define regions related to hand movement. In the main session, participants wore a data glove on their right hand and controlled an on-screen cursor by moving the right fingers. The cursor position was calculated from a predefined hand-to-cursor mapping which was calibrated for individual participants (see Methods). Their goal in the experiment was to reach a target with a cursor as quickly as possible. Participants performed the task under two different conditions alternately (Fig. 1A). In the continuous visual feedback condition, continuous online visual feedback was provided as the position of a on-screen cursor. Additionally, a target appeared red when reached by a cursor. In the other discrete visual feedback condition, the online cursor position was not provided and thus the target color, which appeared red when reached, was the only cue available on the screen. The hand-to-cursor mapping was identical in both feedback conditions.

To quantify how much participants learned a motor skill through the experiment, we formulized success rate as a proportion of time during which a target turned red in a trial. For example, a success rate of 0.1 indicates that participants spent 3.6 seconds to reach a target and stayed in the target for 0.4 seconds. The higher the success rate indicates the faster participants reached the target, which implies participants have learned the hand-to-cursor mapping. As expected, they gradually learned the task throughout the experiment with significant improvement of the success rate from the first run to the last run both in the continuous feedback condition ($t(23) = 13.33$, $p < 10^{-4}$) and in the discrete feedback condition ($t(23) = 4.49$, $p < 0.001$) (Fig. 1B). The improvement of the success rate was 2 to 2.5 times higher in the continuous feedback condition than in the discrete one ($t(23) = 13.97$ $p < 10^{-4}$) (Fig. 1C), confirming that participants learned faster when online cursor feedback is provided.

Activation in sensorimotor and visual cortices

To understand distinct roles of sensorimotor cortices in acquiring a novel motor skill with the two visual feedback conditions, we contrasted fMRI activity between the conditions using a conventional GLM analysis. Notable, we defined regions of interest in the sensorimotor cortices on the cortical surface for all the analyses in the present study since the surface-based analysis improves the specificity of fMRI activity across folded cortical regions over the volume-based analysis[13]. In particular, the surface-based analysis is critical to dissociate fMRI activity between the primary motor (M1) and somatosensory corttices (S1), which are few millimeters apart in 3D volume space, i.e., Euclidean space. In addition, we focused our analyses on the contralateral (left) hemisphere.

The cortical surface-based GLM analysis revealed that the dorsal premotor cortex (PMd) and higher-order visual cortices in the dorsal and the ventral visual pathways exhibited significantly higher fMRI activity in the continuous feedback condition than in the discrete one. In contrast, S1 and early visual areas demonstrated significantly higher fMRI activity when the discrete feedback was provided. M1 is an intermixed region where the activation levels were similar between the conditions (Fig. 2C). It is notable that the activity in S1 and part of M1 is contralateral, meaning that we do not observe it on the right hemisphere, whereas all the other activation patterns are bilateral.

To analyze regional specificity of fMRI activity in the sensorimotor cortices modulated by the visual feedback, we defined 26 rectangular searchlights across sensorimotor cortices related to finger movement (see Methods). The activation was elevated in BA6 (PMd: dorsal premotor) in the continuous feedback condition. However, there was a reversal of the fMRI activity pattern between BA4a (anterior M1) and BA4p (posterior M1), with activation being higher in BA3a, 3b, 1 and 2 (S1) for the discrete feedback condition. Indeed, ROI analysis found fMRI activity, which was higher in BA4a for the continuous feedback ($t(23)=2.50$, $p<0.05$), and higher in BA4p for the discrete feedback ($t(23)=-2.34$, $p<0.05$) (Fig. 2E). While the overall fMRI activity in the sensorimotor cortices was comparable ($F(2, 46)=1.86$, $p=0.166$), there was nearly significant difference between the feedback condition ($F(1, 23)=4.24$, $p=0.51$). Importantly, we found clear double dissociation of the fMRI activity between the feedback conditions across three representative ROIs, PMd, M1, and S1. The activity was higher in motor cortices (PMd and M1) for the continuous feedback ($t(23)=3.68$, $p<0.01$) and was higher in somatosensory cortices (S1) for the discrete feedback ($t(23)=4.38$, $p<0.001$), resulting in significant interaction, effect between ROIs and feedback conditions ($F(1, 23)=184.28$, $p<10^{-4}$).

Interestingly, a similar double dissociation of fMRI activity was also found in the visual cortices (Fig. 2B). While the overall activity across ROIs in the visual cortices (Early visual area, V3AB and V7; $F(1, 23)=3.45$, $p>.05$) was comparable, it was significantly different between the feedback conditions ($F(1, 23) = 29.74$, $p<0.001$). The early visual areas (V1, V2, and V3) were more activated when participants could not see the online cursor movement ($t(23)=2.71$, $p<0.05$); however, V3AB and V7 showed higher activation for the continuous feedback condition ($t(23)=3.46$, $p<0.01$; $t(23)=11.98$, $p<0.001$, respectively) (Fig. 2D), resulting highly significant interaction effect between ROIs and feedback conditions ($F(1, 23)=97.60$, $p<0.001$). Generally, early visual areas were more activated with the discrete feedback, whereas higher-order visual areas were more activated with the continuous feedback.

Connectivity between sensorimotor and visual cortices

Next, we examined whether the connectivity between sensorimotor and visual networks could explain *de novo* visuomotor skill learning. We hypothesized that the connectivity would decrease as learning a hand-to-cursor mapping progressed with increasing autonomy of each network[1]. Furthermore, we sought to find which specific sensorimotor or visual regions are involved in *de novo* skill learning. To define nodes for connectivity analysis, we first chose the top five largest clusters related to finger movement in the sensorimotor and visual cortices and then split the largest motor cortices into two regions, resulting in three regions for each sensorimotor (PMd, M1, and S1) and visual (dorsal, ventral, early) network (Fig. 3A). We focused on connectivity of nodes between sensorimotor network and visual networks, instead of connectivity within each network. The connectivity patterns were comparable with coactivation patterns shown in Fig. 2. Specifically, we found high connectivity between motor cortices (PMd and M1) and the late visual regions (dorsal and ventral) in comparison to connectivity between the motor cortices and the early visual region regardless of conditions or fMRI runs ($t(23)=10.76$, $p<10^{-4}$ for the continuous feedback condition and the first run; $t(23)=10.33$, $p<10^{-4}$ for the continuous feedback condition and the last run; $t(23)=10.89$, $p<10^{-4}$ for the discrete feedback condition and the first run; $t(23)=10.11$, $p<10^{-4}$ for the discrete feedback condition and last first run). In addition, we also figured out higher connectivity between S1 and the early visual region than connectivity between S1 and the late visual regions in the first run of the continuous feedback ($t(23)=4.07$, $p<0.001$). It is noteworthy that in the continuous feedback condition, coactivated regions include the motor cortices and late visual areas, whereas the discrete feedback condition exhibited coactivation between S1 and the early visual region.

To investigate change in connectivity over time, we performed a paired t-test. As a result, the connectivity between S1 and early visual region during the continuous feedback condition significantly decreased from the first to the last fMRI run ($t(23)=5.12$, Bonferroni-corrected, $p<0.001$) (Fig. 3B). All the other connectivity did not reach significance level of corrected $p<0.05$ for 18 tests (connectivity between three sensorimotor ROIs and three visual ROIs for each feedback condition). A subsequent linear mixed effects model analysis (fixed effect: four fMRI runs, random effect: participants) further revealed that the decreased of connectivity between S1 and early visual region is related to performance improvement (coef = -0.36, SE= 0.077, $p<0.001$) (Fig. 3C).

Discussion

In this work, we found distinctive involvement of the sensorimotor and visual cortices subregions in learning a motor skill *de novo*. We found clear double dissociation of fMRI activity in the subregions as well as their interaction, which were mediated by visual feedback. Motor cortices and late visual cortices were more activated when continuous visual feedback is available than when only binary visual feedback is available. In contrast, somatosensory cortices and early visual cortices exhibited the opposite activation pattern. We also found significant learning-

induced reduction of connectivity between somatosensory and earl visual cortices, which is correlated with improved performance.

It is challenging to separate fMRI activity between motor and somatosensory cortices since efferent motor commands and afferent proprioceptive feedback are processed simultaneously during continuous motor control[7]. In our experiment, manipulation of visual feedback allowed us to dissociate the fMRI activity by modulating the extent to which participants depended on visual or proprioceptive feedback to perform the task. When visual feedback is limited as binary feedback, participants were more likely attend to proprioception, i.e., hand posture, leading to higher fMRI activity in somatosensory cortices than in motor cortices. That is, the extent of visual feedback, full online or binary feedback switches attentional focus on the visual or proprioceptive modality as suggested in a previous study[11]. In our experiment of learning an arbitrary hand-to-cursor mapping, this dissociation would be more prominent than in typical motor learning tasks due to larger uncertainty about motor and sensory goals of the task[7]. We found the boundary of the dissociation in the primary motor cortex. Specifically, the anterior part showed greater activation with the presence of online feedback compared to its absence, while the posterior part exhibited the reverse pattern. Our results are consistent with other studies claiming that the anterior M1 is more involved in motor execution which is externally triggered and the posterior M1 is more related to increased sensory attention[14,15]. Indeed, the anterior and posterior M1 were known to differ not only in their cytoarchitecture and neurochemistry but in their function[16-18]. Although our surface-based GLM analysis has advantage over a volume-based GLM to delineate the boundary with less overlapped fMRI activity between M1 and S1[15], the spatial resolution would not be enough to clearly dissociate the functional difference. Future studies using 7 T fMRI with better spatial resolution and SNR would be necessary to clearly dissociate roles of sensorimotor subregions.

The task-based functional connectivity analysis further explains computational processes involved in *de novo* motor skill learning. Recent research has sparked debate around two contrasting motor control theories: the optimal control theory and the active inference theory[19]. A key point of contention lies in the active inference theory's rejection of the concept of efference copy. Based on our results, we claim that the optimal control theory is more plausible explanation for *de novo* motor skill learning than the active inference theory, which is a Bayesian model requiring prior knowledge that participants do not have when learning a motor skill from scratch. If the optimal control theory governs *de novo* motor skill learning, it suggests that M1 transmits an efference copy to the parietal cortex[20]. Notably, we found consistent and strong connection between M1 and the dorsal visual region in the parietal cortex. Furthermore, our primary finding of a clear dissociation between M1 and S1 also supports the optimal control theory, as it contradicts the active inference theory's premise that action and perception cannot be separated[21]. Our claim aligns with an earlier study suggesting that S1 plays a role in receiving an efference copy as it encodes sensory information in anticipation of movements[22]. Future studies may be warranted to reconcile between these two explanations for *de novo* motor learning.

A landmark fMRI study in motor skill learning revealed that visuomotor interaction is more dominant in earlier stage of learning visuomotor mappings but decreases in later stage of learning with more automatic performance[1]. Our results demonstrated more detailed patterns of interaction between sensorimotor and visual subregions, highlighting more significant

contribution of S1 and early visual cortex to learning a *de novo* motor skill. The more significant contribution of the early instead of late visual cortex would be related to localizing visual fields corresponding to target positions. However, the current experiment does not provide clear explanation about lack of contribution of the interaction between motor cortices and late visual cortices to motor learning. We only speculate that the somatosensory cortex could play a more important role in initial visuomotor learning when a sensory target is highly uncertain[2] as in our task learning an arbitrary hand-to-cursor mapping. It would be intriguing to explore the contribution of S1 to *de novo* motor learning in more advanced stage of learning with a longitudinal study[12].

Materials and Methods

Subjects

Twenty-six healthy adults from Sungkyunkwan University community participated in this study. According to the Edinburgh Handedness Inventory[23], all participants were right-handed. In addition, they had no history of neurological or psychiatric disease and had normal or corrected-to-normal vision. Twenty-four participants (14 females; mean age = 24.9 $\pm$ 4.7 years, age range = 18-35 years) completed all the experiment sessions. Two participants dropped out in the middle of the experiment due to severe fatigue, and thus their data were excluded from the analysis. All participants were provided written consent in accordance with the dictates of the trust ethics committee of Sungkyunkwan University, Suwon, Republic of Korea. Participants underwent two scanning sessions for 1.5 hours at a 3T fMRI scanner and received monetary reward for their participation after the experiment.

fMRI data collection

In the present study, fMRI data was acquired using a 3-T Siemens Magnetom Prisma scanner equipped with a 64-channel head coil. Functional images were obtained using an echo-planar imaging (EPI) sequence with specific parameters: a total of 300 volumes (with 310 volumes for localizer fMRI), a repetition time (TR) of 2,000 ms, an echo time (TE) of 35.0 ms, a flip angle (FA) of 90°, a field of view (FOV) measuring 200 mm, a matrix size of 101 X 113 X 91 voxels, 72 axial slices, and a slice thickness of 2.0 mm. For anatomical referencing, a T1-weighted anatomical scan of the entire brain was conducted using a magnetization-prepared rapid acquisition with gradient echo MPRAGE sequence. This anatomical scan employed specific parameters, including a TR of 2,300 ms; a TE of 2.28 ms; a FA of 8°; an FOV of 256 mm; a matrix size of 204 X 262 X 260 voxels; 192 axial slices; and a slice thickness of 1.00 mm. Before the functional scans, two EPI images were acquired with opposite-phase encoding directions (posterior-to-anterior and anterior-to-posterior) to enable subsequent distortion correction.

Data glove

Participants wore the MR-compatible data glove (5DT Glove 14 Ultra) on their right hand. With the data glove, hand postures recorded by 14 sensors were converted to cursor positions on the 2-dimensional screen. The hand-to-cursor mapping is defined as below.

$$\begin{bmatrix} x \\ y \end{bmatrix} = \begin{bmatrix} a_{x,1} & a_{x,2} & a_{x,3} & \cdots & a_{x,14} \\ a_{y,1} & a_{y,2} & a_{y,3} & \cdots & a_{y,14} \end{bmatrix} \times \begin{bmatrix} s_1 & s_2 & s_3 & \cdots & s_{14} \end{bmatrix}^T + \begin{bmatrix} x_0 \\ y_0 \end{bmatrix}$$

where $s_k (k = 1,2, \ldots ,14)$ indicates each of the 14 sensor inputs from the data glove, and x and y indicate the horizontal and vertical position of the cursor. The timeseries data of the 14 sensors was sampled at 60 Hz. The above equation can be rewritten as $\mathbf{r} = \mathbf{A}\mathbf{s} + \mathbf{r_0}$, where the mapping matrix $\mathbf{A}$ and the offset $\mathbf{r_0}$ were determined from the calibration and localizer session.

Calibration

Before fMRI scanning, participants had a calibration phase in an MRI scanning control room. After wearing the data glove, participants moved their right hands while they could see a graph of 14 bars moving in real-time based on the 14 sensors. Participants were instructed to try various combinations of hand postures. Next, we conducted principal component analysis with the covariance matrix derived from the time series collected from the 14 sensors. The first two principal components were employed to create the mapping matrix $\mathbf{A}$, and the offset $\mathbf{r_0}$ was calculated to ensure that the average hand posture was aligned with the center of the screen. After that, we ensured if participants could visit all 25 cells of a 5×5 grid (Fig. 1A).

Localizer session

After the calibration phase, participants moved to an MRI scanning room. They lay on their back in the scanner, observing the screen via a mirror. To reduce head movement, foam pads were applied to all participants. In addition, they wore the data glove on their right hand and put the hand in a comfortable position. Notably, participants could not see their hand moving during the entire fMRI experiment.

To localize finger movement regions in the brain, participants had a localizer session before the main task session. When "Move" was displayed on the screen, participants performed natural-speed movements with their right fingers, ceasing their movements upon the appearance of the "Stop" text. Each "Move" or "Stop" condition had a duration of 48 seconds, separated by 2-second intervals, and a total of six sets of "Move" and "Stop" conditions were executed. To make sure it is de novo learning to participants, we recalibrated the mapping matrix $\mathbf{A}$ and the offset $\mathbf{r_0}$ using the data acquired from the finger movements in the last two "Move" blocks. We also ensured that all 25 grid cells were reachable by finger movements.

Main task session

Participants were required to move their right fingers to control a cursor, and to reach a target cell. A target cell is a gray cell with a yellow crosshair in its center. If participants reached a target cell, its color changed to red, and they were required to stay in the target cell until the next one appeared. In other words, the goal of the main task for participants was to reach a target as quickly as possible and to stay as long as possible in the target. A target cell appeared

for 4 s. Regardless of whether participants reached a target or not, the target was changed to another one after 4 s of 1 trial. 1 block had 12 trials with a sequence of either 13-3-25-21-13-25-3-21-25-13-21-3 (Sequence 1: triangle) or 13-23-5-1-13-5-23-1-5-13-1-23 (Sequence 2: inverted triangle), where the number indicates the grid cell number determined by the formula $k = 5i + j - 5$, with i representing the row index and j representing the column index. Half of participants were presented with Sequence 1 and the other half were presented with Sequence 2 for counterbalancing. In total, there were 4 runs and each run consisted of 12 blocks. Thus, the duration of each run was about 576 s (144 trials × 4 s).

Notably, there were two experimental conditions: full visual feedback and discrete visual feedback. In the full visual feedback condition, participants could see both cursor movement and targets. On the other hand, in the discrete visual feedback condition, participants could only see targets, but the cursor was not visible (Fig. 1B). Thus, participants could only guess their cursor position by the color of targets. The two conditions were applied in separate blocks alternately. During odd-numbered blocks the cursor position was continuously represented by a white crosshair, whereas it was hidden during even-numbered blocks.

Behavioral data analysis

The proportion of time during which a target turned red was measured as a trial-by-trial success rate. For example, the success rate of one block was defined by the amount of time targets turned red during one block divided by 48 s, a total time of one block. We used two-sided paired t-test between different conditions or runs to see if there was significant difference. MATLAB (version R2022a, MathWorks), Python (version 3.10.8), and Jupyter notebook (version 6.4.12) were utilized for all statistical analysis.

fMRI data analysis: preprocessing

MRI data were analyzed with FreeSurfer (version 7.2.0)[24]. We first followed the FreeSurfer 'recon-all' pipeline for preprocessing of anatomical data. Then for functional data, we followed FreeSurfer Functional Analysis Stream (FS-FAST) preprocessing pipeline https://surfer.nmr.mgh.harvard.edu/fswiki/FsFastTutorialV6.0/FsFastPreProc). Functional data from each subject were registered to the same-subject FreeSurfer anatomical data with motion correction and slice-timing correction. Then the functional data were resampled to common FreeSurfer space. Note that we didn't do spatial smoothing, because first we wanted to investigate precise brain mapping to distinguish sensorimotor areas, and second non-smoothed data were used for connectivity analysis.

fMRI data analysis: GLM

We utilized FS-FAST for the GLM analysis[25]. We utilized FS-FAST for the GLM analysis. To identify regions responding to full visual feedback and only discrete visual feedback, we used blocked task design for the regressors of interest. Then the regressors of interest were convolved with the SPM canonical hemodynamic response function (HRF) of zero derivatives. It was not smoothed here as well. For nuisance regressors, we used motion parameters created in preprocessing. The top three components were used. In addition, third order polynomial regressors were included. After the first-level analysis, individual results were concatenated into one file with the "isxconcat-sess" function. Then group GLM was performed with "mri_glmfit".

Multiple comparisons correction was done by “mri_glmfit-sim” with cluster-forming threshold (CFT) of $p < 10^{-4}$ and cluster-wise p-value of $p < .05$. The final full width at half maximum (FWHM) of the inherent smoothness was taken into account for multiple comparisons correction. Similar analysis was also done to the Localizer result with different conditions of “Move” and “Stop” to identify regions responding to hand movement.

ROI selection

We defined ROIs in PMd, M1, S1, V1, V2, V3, V3A, V3B and V7 based on the GLM result. ROIs in sensorimotor areas were defined as an overlap between clusters obtained from the localizer result and Brodmann areas provided by FreeSurfer[26] (BA6 for PMd; BA4a and 4p for M1; BA1, 2, 3a and 3b for S1) For visual areas, we used the atlas made by Wang, et al[27]. For precise brain mappings, we subdivided sensorimotor areas. We first flattened the fsaverage brain. Then we cut the ROIs at regular distances as parallel as possible to the boundaries between the ROIs (Fig. 2E).

For connectivity analysis, we chose the 5 biggest clusters made from the GLM result (Fig. 3A). On the other hand, based on our hypotheses, we divided the yellow cluster into PMd and M1 parts. We also used only the posterior part of the scarlet cluster and defined it as a dorsal visual cluster. As a result, we have 6 clusters of PMd, M1, S1, dorsal visual, ventral visual and early visual areas.

fMRI data analysis: connectivity

Using “mri_surfcluster”, we figured out each vertex number from the 6 clusters with the highest beta estimates for each participant. Then each participants’ circular masks of 3 mm radius were drawn around the vertices with the “mri_volsynth”, “mris_fwhm”, and “mri_binarize” functions. Timeseries data within the masks were averaged and extracted by “mri_segstats”. Finally, we regressed out the same motion parameters and third order polynomials as used in the GLM analysis as well as other nuisance variables such as global signal, white matter, ventricles and cerebrospinal fluid (VCSF). White matter, ventricles and VCSF regressors were obtained by “fcseed-sess” using the PCA option, and the top one component was used. Then partial correlations between the two seeds were calculated with covariances of both conditions which are convolved with the SPM HRF.

References

1 Bassett, D. S., Yang, M., Wymbs, N. F. & Grafton, S. T. Learning-induced autonomy of sensorimotor systems. *Nat Neurosci* **18**, 744-751, doi:10.1038/nn.3993 (2015).

2 Ostry, D. J. & Gribble, P. L. Sensory Plasticity in Human Motor Learning. *Trends Neurosci* **39**, 114-123, doi:10.1016/j.tins.2015.12.006 (2016).

3 Izawa, J. & Shadmehr, R. Learning from sensory and reward prediction errors during motor adaptation. *PLoS Comput Biol* **7**, e1002012, doi:10.1371/journal.pcbi.1002012 (2011).

4 Therrien, A. S., Wolpert, D. M. & Bastian, A. J. Effective reinforcement learning following cerebellar damage requires a balance between exploration and motor noise. *Brain* **139**, 101-114, doi:10.1093/brain/awv329 (2016).

5 Telgen, S., Parvin, D. & Diedrichsen, J. Mirror reversal and visual rotation are learned and consolidated via separate mechanisms: recalibrating or learning de novo? *J Neurosci* **34**, 13768-13779, doi:10.1523/JNEUROSCI.5306-13.2014 (2014).

6 Ossmy, O. & Mukamel, R. Behavioral and neural effects of congruency of visual feedback during short-term motor learning. *Neuroimage* **172**, 864-873, doi:10.1016/j.neuroimage.2017.12.020 (2018).

7 Bernardi, N. F., Darainy, M. & Ostry, D. J. Somatosensory Contribution to the Initial Stages of Human Motor Learning. *J Neurosci* **35**, 14316-14326, doi:10.1523/JNEUROSCI.1344-15.2015 (2015).

8 Ogawa, K., Inui, T. & Sugio, T. Separating brain regions involved in internally guided and visual feedback control of moving effectors: an event-related fMRI study. *Neuroimage* **32**, 1760-1770, doi:10.1016/j.neuroimage.2006.05.012 (2006).

9 Schmitter, C. V., Steinstrater, O., Kircher, T., van Kemenade, B. M. & Straube, B. Commonalities and differences in predictive neural processing of discrete vs continuous action feedback. *Neuroimage* **229**, 117745, doi:10.1016/j.neuroimage.2021.117745 (2021).

10 Mayhew, S. D., Porcaro, C., Tecchio, F. & Bagshaw, A. P. fMRI characterisation of widespread brain networks relevant for behavioural variability in fine hand motor control with and without visual feedback. *Neuroimage* **148**, 330-342, doi:10.1016/j.neuroimage.2017.01.017 (2017).

11 Limanowski, J. & Friston, K. Attentional Modulation of Vision Versus Proprioception During Action. *Cereb Cortex* **30**, 1637-1648, doi:10.1093/cercor/bhz192 (2020).

12 Choi, Y., Shin, E. Y. & Kim, S. Spatiotemporal dissociation of fMRI activity in the caudate nucleus underlies human de novo motor skill learning. *Proc Natl Acad Sci U S A* **117**, 23886-23897, doi:10.1073/pnas.2003963117 (2020).

13 Brodoehl, S., Gaser, C., Dahnke, R., Witte, O. W. & Klingner, C. M. Surface-based analysis increases the specificity of cortical activation patterns and connectivity results. *Sci Rep* **10**, 5737, doi:10.1038/s41598-020-62832-z (2020).

14 Binkofski, F. *et al.* Neural activity in human primary motor cortex areas 4a and 4p is modulated differentially by attention to action. *J Neurophysiol* **88**, 514-519, doi:10.1152/jn.2002.88.1.514 (2002).

15 Alahmadi, A. A. S. Functional network analysis of the sub-regions of the primary motor cortex during rest. *Neuroreport* **31**, 691-695, doi:10.1097/WNR.0000000000001470 (2020).
16 Geyer, S. *et al.* Two different areas within the primary motor cortex of man. *Nature* **382**, 805-807, doi:10.1038/382805a0 (1996).
17 Tomasino, B. & Gremese, M. The Cognitive Side of M1. *Front Hum Neurosci* **10**, 298, doi:10.3389/fnhum.2016.00298 (2016).
18 Rathelot, J. A. & Strick, P. L. Subdivisions of primary motor cortex based on cortico-motoneuronal cells. *Proc Natl Acad Sci U S A* **106**, 918-923, doi:10.1073/pnas.0808362106 (2009).
19 Adams, R. A., Shipp, S. & Friston, K. J. Predictions not commands: active inference in the motor system. *Brain Structure and Function* **218**, 611-643 (2013).
20 Sirigu, A. *et al.* The mental representation of hand movements after parietal cortex damage. *Science* **273**, 1564-1568 (1996).
21 Baltieri, M. & Buckley, C. L. in *Artificial life conference proceedings.* 121-128 (MIT Press One Rogers Street, Cambridge, MA 02142-1209, USA journals-info …).
22 Sun, H. *et al.* Sequential activation of premotor, primary somatosensory and primary motor areas in humans during cued finger movements. *Clinical Neurophysiology* **126**, 2150-2161 (2015).
23 Oldfield, R. C. The assessment and analysis of handedness: the Edinburgh inventory. *Neuropsychologia* **9**, 97-113, doi:10.1016/0028-3932(71)90067-4 (1971).
24 Dale, A. M., Fischl, B. & Sereno, M. I. Cortical surface-based analysis. I. Segmentation and surface reconstruction. *Neuroimage* **9**, 179-194, doi:10.1006/nimg.1998.0395 (1999).
25 Burock, M. A. & Dale, A. M. Estimation and detection of event-related fMRI signals with temporally correlated noise: A statistically efficient and unbiased approach. *Human brain mapping* **11**, 249-260 (2000).
26 Fischl, B. *et al.* Cortical folding patterns and predicting cytoarchitecture. *Cerebral cortex* **18**, 1973-1980 (2008).
27 Wang, L., Mruczek, R. E., Arcaro, M. J. & Kastner, S. Probabilistic Maps of Visual Topography in Human Cortex. *Cereb Cortex* **25**, 3911-3931, doi:10.1093/cercor/bhu277 (2015).

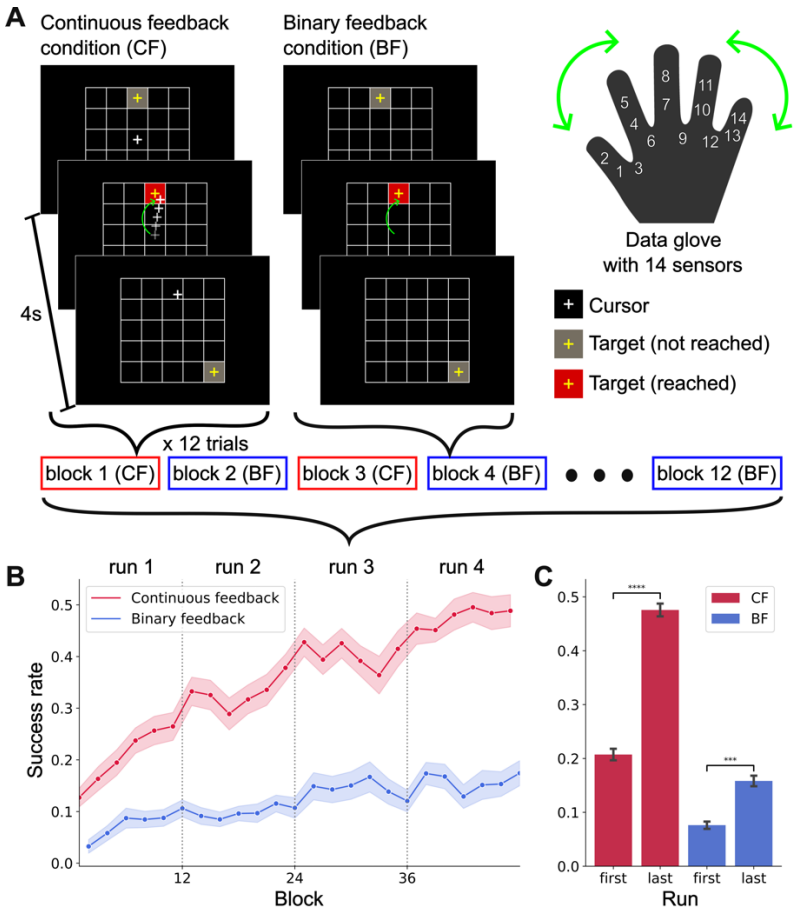

Figure 1 (A) Overview of the *de novo* motor learning task. Participants learned to control a cursor by moving their right fingers. Their goal was to reach a target on a 5 x 5 grid as quickly as possible and stayed on the target until the next target is turned on. There were two types of conditions: continuous feedback condition and binary feedback condition. In the continuous feedback condition, participants could see both cursor movement and a target, whereas cursor movement was hidden in the binary feedback condition. **(B)** Behavioral result of the task on the continuous feedback condition and the binary feedback condition. The increase in success rate implies that participants reached the targets more quickly and stayed on them longer. Participants performed better with the continuous feedback. **(C)** Averaged success rates of the first and the last run from both conditions. Success rates significantly increased in both conditions, meaning that they also learned the mapping in the binary feedback condition.

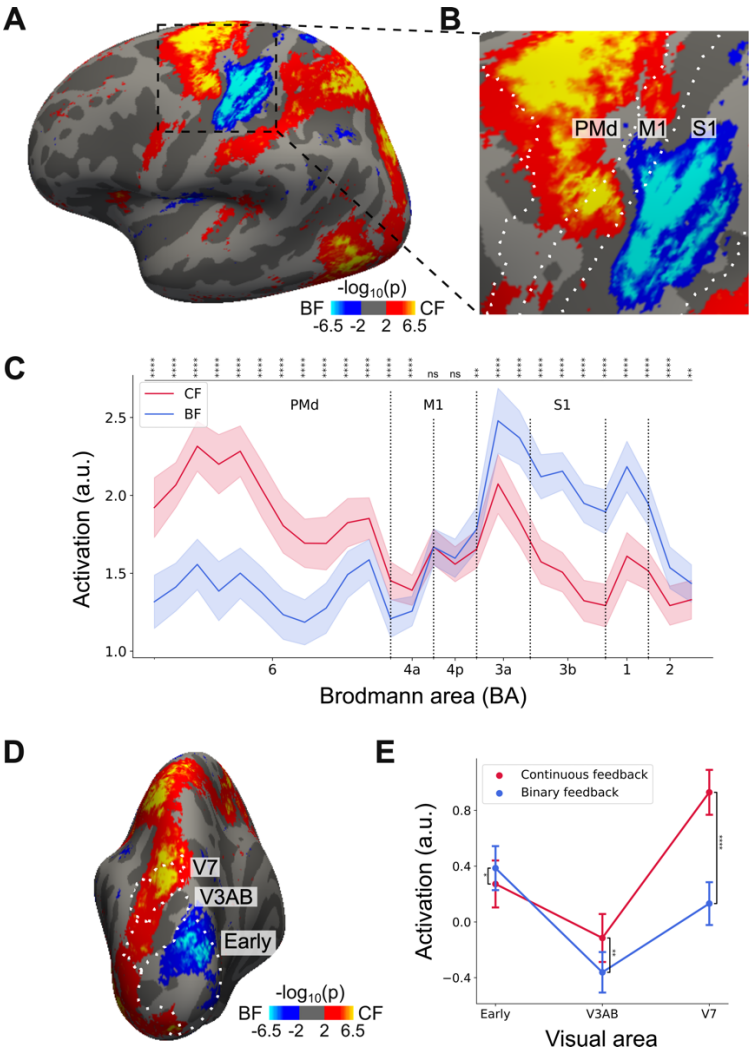

Figure 2 (A) Univariate activation map from the lateral view for the contrast continuous feedback > binary feedback. **(B)** Enlarged map for (A) highlighting sensorimotor regions. **(C)** ROI analysis (see Methods) of mean activation (± standard error of mean). **(D)** Same as A but from the caudal view. **(E)** ROI analysis of mean activation over visual areas (± standard error of mean). The level of significance was represented by asterisks as follows. *p<0.05, **p<0.01, ***p<0.001, ****p<10^{-4}

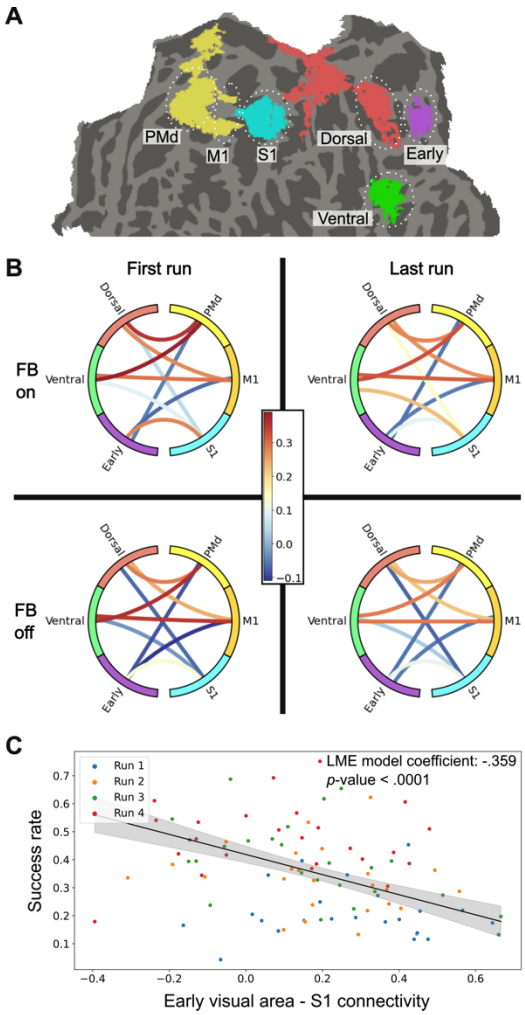

Figure 3 (A) Top 5 significant clusters from the GLM result. The yellow cluster was parcellated into PMd and M1. Only posterior part of the violet cluster was used and defined as dorsal visual region. **(B)** Functional connectivity across sensorimotor regions and visual regions. **(C)** The relationship between S1-early visual cortex connectivity and the success rate. Linear mixed effect model was used to take account of individual differences in motor skill learning.